IEEE Access
Multidisciplinary | Rapid Review | Open Access Journal

Received January 9, 2018, accepted February 12, 2018, date of publication February 21, 2018, date of current version April 18, 2018.

Digital Object Identifier 10.1109/ACCESS.2018.2807700

An Automatic Cardiac Arrhythmia Classification System With Wearable Electrocardiogram

YUFA XIA[1], HUAILING ZHANG[2], LIN XU[3], ZHIFAN GAO[1], (Member, IEEE), HEYE ZHANG[1], (Member, IEEE), HUAFENG LIU[4], AND SHUO LI[5]

[1]Shenzhen Institutes of Advanced Technology, Chinese Academy of Sciences, Shenzhen 518055, China
[2]School of Information Engineering, Guangdong Medical University, Dongguan 523808, China
[3]Department of Cardiology, General Hospital of Guangzhou Military Command of PLA, Guangzhou 510000, China
[4]State Key Laboratory of Modern Optical Instrumentation, Department of Optical Engineering, Zhejiang University, Hangzhou 310027, China
[5]Western University, London, ON N6A 3K7, Canada

Corresponding authors: Huailing Zhang (huailing@163.com) and Zhifan Gao (zf.gao@siat.ac.cn)

This work was supported in part by the National Key Research and Development Program of China under Grants 2016YFC1301700 and 2017YFE0104000, in part by the Shenzhen Dual Chain Funding under Grant 20170502171625936, in part by the National Natural Science Foundation of China under Grants 61771464 and 61427807, in part by the Science and Technology Planning Project of Guangdong Province under Grants 2014A020212257 and 2013A022100036, in part by the Guangzhou Science and Technology Planning Project under Grant 201704020079, in part by the Shenzhen Innovation Funding under Grants JCYJ20151030151431727, JCYJ20150401145529007, and SGLH20161212104605195, and in part by the China Postdoctoral Science Foundation under Grant 2017M620394.

ABSTRACT This paper presents an automatic wearable electrocardiogram (ECG) classification and monitoring system with stacked denoising autoencoder (SDAE). We use a wearable device with wireless sensors to obtain the ECG data, and send these ECG data to a computer with Bluetooth 4.2. Then, these ECG data are classified by the automatic cardiac arrhythmia classification system. First, the ECG feature representation is learned by the SDAE with sparsity constraint. Then, the softmax regression is used to classify the ECG beats. In the fine-tuning phase, an active learning is added to improve the performance. In the active learning phase, we use the method that relies on the deep neural networks posterior probabilities to associate confidence measures to select the most informative samples. Breaking-ties and modified breaking-ties methods are used to select the most informative samples. We validate the proposed method on the well-known MIT-BIH arrhythmia database and ECG data obtained from the wearable device. We follow the recommendations of the Association for the Advancement of Medical Instrumentation for class labeling and results presentation. The results show that the classification performance of our proposed approach outperforms the most of the state-of-the-art methods.

INDEX TERMS Stacked denoising autoencoder, wearable device, active learning, breaking-ties, modified breaking-ties.

I. INTRODUCTION

ECG abnormality plays a significant role in the prediction of cardiovascular diseases (CVDs) events in both young and old population [1], [2]. As the abnormality of the ECG is an intermittent symptom, the arrhythmia beat may not emerge in a short time. This causes that the diagnosis of ECG in the hospital is limited. Moreover, the traditional ECG monitoring system often connects the individuals and the instrument with a signal line; and the direct-wired connection confines the ECG monitoring. While, the wearable device with wireless sensors could monitor the cardiac activity without influencing the user's daily life [3], [4]. The wearable device with wireless sensors could generate a large amount of data easily. Although the anomaly of ECG waveform in the heart rate or rhythm or change in the morphological pattern can be confirmed easily by an expert cardiologist, it may be infeasible to inspect each heartbeat among the large number of ECG data for clinician.

To overcome the issue, automatic methods are proposed to classify the ECG. Recently, several approaches were utilized for automatic ECG classification, such as frequency analysis [5], k-Nearest Neighbor clustering [6], mixture-of-experts method [7], Classification and Regression Trees [8], [9], Artificial Neural Networks [10], Hidden Markov Models [11], support vector machines (SVM) [12], Probabilistic Neural Networks [13], recurrent NN (RNN) [14] and path forest [15].

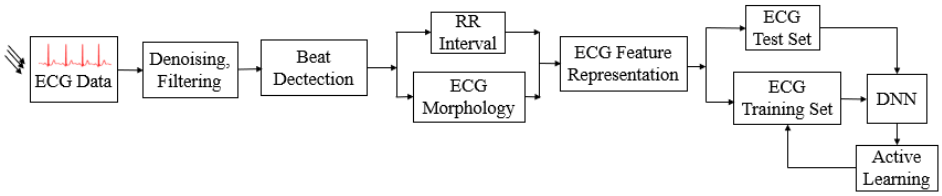

FIGURE 1. Overview of the proposed approach.

Despite the great task that the automatic ECG assessment approaches have been done, in practice, these methods do not perform well due to some reasons. Firstly, the ECG signals can be contaminated by various kinds of noise and physiological artifact, such as baseline wanders, power line interference, and muscle contraction. The noise and physiological artifact make the assessment of ECG difficult in automatic computerized approach. Moreover, the inter-individual variations of the ECG signals can make the methods have an inconsistent performance when they are used to classify different subjects. In addition, the time-varying dynamics and morphological characteristics of ECG signals in the same subject can also increase the difficulty of the automatic assessment [16].

Furthermore, there is another severe problem. When assessing and testing a particular method on a benchmark dataset, it is lack of application of the common practice. For this reason, the standards and recommended practices for performance results of automated arrhythmia detection algorithms are provided by the Association for the Advancement of Medical Instrumentation (AAMI) [17]. Explicitly, the AAMI defines five heartbeat classes: normal (N), ventricular (V), supraventricular (S), fusion of normal and ventricular (F) and unknown beats (Q). However, only few studies have used AAMI standards to classify the ECG in automatic approaches [18]–[21].

The afore-mentioned ECG classification systems use traditional methods or shallow neural networks. Compared with shallow architectures (i.e., handcrafted features fed as input to a kernel classifier), deep learning extracts the feature representation automatically from the input data. Deep belief networks (DBNs) [22], stacked auto-encoder (SAE) [23], convolutional neural networks (CNNs) [24] are three typical deep learning architectures. For the automatic ECG classification, Meng and Zhang [25] proposed an approach based on the combination DBN and SVM. They used DBN to learn feature representation and then fed the features to SVM for training and classification. And Kiranyaz *et al.* [26] proposed a method with 1-D CNN to classify the ECG signals. However, the performance of the classification remains to be improved.

To overcome the above deficiencies, we propose a novel approach to classify ECG signals based on the stacked denoising autoencoder (SDAE) with sparity constraint and softmax regression. Firstly, we use SDAE with sparsity constraint to learn an adequate feature representation. Then we classify the ECG signals according to the AAMI standard by the softmax regression layer. In the fine-tuning phase, we added active learning to improve the classification [27]. The illustration of the proposed approach is shown in Fig 1. Two strategies are used to perform active learning: 1) a criterion called breaking ties (BT) [28], and 2) modified breaking ties (MBT) [29]. In the experiments, we validate our method on two databases. The first database is the well-known MIT-BIH arrhythmia Database. The second database is the arrhythmia data that we obtained by the wearable device.

The rest of this paper is organized as follows. Section II describes the wearable device using to obtain ECG data. In Section III, the SDAE, softmax regression and active learning method are described in detail. The database and experimental results are presented in Section IV. Finally, Section V and Section VI present the discussion and conclusion, respectively.

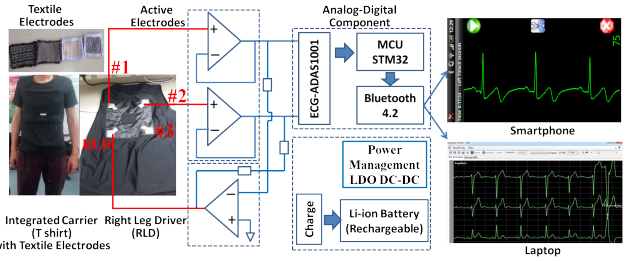

FIGURE 2. The wearable device using to obtain ECG signals.

II. THE WEARABLE DEVICE USING TO OBTAIN ECG DATA

The wearable device using to obtain ECG signals is demonstrated in Fig. 2. It consists of three parts: cloth carrier, biosensor platform, and smart terminals. The cloth carrier is made of elastic fabric for obtaining sufficient adhesion of textile electrodes to the pectoral muscles. The magnetic connector is used to guarantee the connection stability between textile electrodes and hardware platform. In the biosensor platform, the ADI ECG analog front-end (ADAS1001) is used for obtaining the ECG signals. The Microcontroller (STM32) is used to realize the data processing, packing and retransmission to smart terminals via Bluetooth 4.2 protocol. LDO DC-DC regulator with 95% conversion efficiency is introduced for decreasing the power consumption further. As the

ECG signal is weak and easy to be corrupted by multiple noise, we design a digital filter group to reduce the influence of extensive noises for later evaluation.

III. DESCRIPTION OF THE PROPOSED APPROACH

In this paper, SDAE is used to extract ECG feature representation. Then, a softmax regression is utilized to classify ECG with the extracted feature vector. Additionally, active learning is employed to improve the performance in the fine tuning phase. In the next subsections, the details of the proposed approach are described.

A. FEATURE EXTRACTION USING THE SDAE

An autoencoder is an unsupervised learning algorithm that applies back-propagation. As a neural network, the autoencoder consists of three layers, including a visible layer, hidden layer, and reconstruction layer. The three-layered neural network defines a non-linear hypothesis $\boldsymbol{h}_{\boldsymbol{w},\boldsymbol{b}}(\boldsymbol{x}_i)$ with parameters $\boldsymbol{w}$ and $\boldsymbol{b}$ that the data can be fitted. For a set of unlabeled training examples $\{\boldsymbol{x}_i|\boldsymbol{x}_i \in \boldsymbol{R}^n, i = 1, 2, \ldots, m\}$, it attempts to learn an approximation function $\boldsymbol{h}_{\boldsymbol{w},\boldsymbol{b}}(\boldsymbol{x}) \approx \boldsymbol{x}$. In other words, it tries to reconstruct visible layer data in the reconstruction layer. Typically, the autoencoder consists of encoding part and decoding part.

In the encoding part, the input $\boldsymbol{x}_i$ is mapped to the hidden representation $\boldsymbol{h}_i \in \boldsymbol{R}^L$ though a non-linear activation function as follows:

$$\boldsymbol{h}_i = f(\boldsymbol{W}^{(e)} \cdot \boldsymbol{x}_i + \boldsymbol{b}^{(e)}). \tag{1}$$

Where $\boldsymbol{W}^{(e)} \in \boldsymbol{R}^{L\times n}$ is the encoder weight matrix and $\boldsymbol{b}^{(e)} \in \boldsymbol{R}^L$ is the encoder bias vector. Usually, the sigmoid function, i.e. $f(z) = \frac{1}{1+\exp(-z)}$ and tanh function, i.e. $f(z) = \frac{e^z-e^{-z}}{e^z+e^{-z}}$ are used as the activation function. In this paper, we select sigmoid function as the activation function.

In the decoding part, the hidden representation $\boldsymbol{h}_i \in \boldsymbol{R}^L$ reconstructs the input vector $\boldsymbol{x}_i$ through the activation function as follows:

$$\boldsymbol{r}_i = f(\boldsymbol{W}^{(d)} \cdot \boldsymbol{h}_i + \boldsymbol{b}^{(d)}). \tag{2}$$

Where $\boldsymbol{W}^{(d)} \in \boldsymbol{R}^{n\times L}$ is the decoder weight matrix and $\boldsymbol{b}^{(d)} \in \boldsymbol{R}^n$ is the decoder bias vector.

A denoising autoencoder is trying to reconstruct the input from a noisy corrupted input. To reconstruct a robust feature representation, noise is added to input data $\boldsymbol{x}_i \in \boldsymbol{R}^n$. Then the noisy corrupted version $\tilde{\boldsymbol{x}}_i \in \boldsymbol{R}^n$ is used to reconstruct the input $\boldsymbol{x}_i \in \boldsymbol{R}^n$. As the Eq. (1), in the encoding part, the corrupted input $\tilde{\boldsymbol{x}}_i$ is mapped to a hidden representation $\boldsymbol{h}_i = f(\boldsymbol{W}^{(e)} \cdot \tilde{\boldsymbol{x}}_i + \boldsymbol{b}^{(e)})$; and as the Eq. (2), in decoding part, the network reconstructs $\tilde{\boldsymbol{x}}_i = f(\boldsymbol{W}^{(d)} \cdot \boldsymbol{h}_i + \boldsymbol{b}^{(d)})$. To optimize the parameters $(\boldsymbol{w}, \boldsymbol{b}) = (\boldsymbol{W}^{(e)}, \boldsymbol{b}^{(e)}, \boldsymbol{W}^{(d)}, \boldsymbol{b}^{(d)})$, we try to minimize the cost function as follows [30]:

$$J(\boldsymbol{w}, \boldsymbol{b}) = \frac{1}{m}\sum_{i=1}^{m}\left(\frac{1}{2}\left\|\boldsymbol{h}_{\boldsymbol{w},\boldsymbol{b}}(\tilde{\boldsymbol{x}}_i - \boldsymbol{x}_i)\right\|^2\right) + \frac{\lambda}{2}\sum_{l=1}^{n_l-1}\sum_{i=1}^{s_l}\sum_{j=1}^{s_l+1}\left(w_{ji}^{(l)}\right)^2. \tag{3}$$

Where the n_l is the number of layers in the network; the s_l denotes the number of hidden layer nodes. The first term in Eq. (3) is the average sum-of-squares error term. The second term denotes a regularization term (also called a weight decay term) that tends to decrease the magnitude of the weight, and help prevent overfitting. The λ controls the penalty term facilitating weight decay.

In the denoising autoencoder with sparsity constraint, a sparsity constraint is imposed on the hidden nodes. When a sparsity constraint is forced on the hidden nodes, the autoencoder can detect interesting structure in the data, even if the number of hidden units is large [31]. To enforce the neurons to be inactive most of the time, $\boldsymbol{h}_j(\boldsymbol{x}_i)$ denotes the activation of the jth hidden node, and the average activation of hidden node j is denoted as:

$$\hat{\rho}_j = \frac{1}{m}\sum_{i=1}^{m}\boldsymbol{h}_j(\boldsymbol{x}_i). \tag{4}$$

To constrain sparity, we enforce the $\hat{\rho}_j = \rho$. Where ρ is a sparsity parameter, which is a small positive value close to zero. To achieve this, we will add an extra penalty term to our optimization objective that penalizes $\hat{\rho}_j$ deviating significantly from ρ. Many choices of the penalty term will give reasonable results. We choose the Kullback–Leibler (KL) divergence similarity between $\hat{\rho}_j$ and ρ:

$$J_{KL}(\rho\|\hat{\rho}) = \sum_{j=1}^{n'}\rho log\frac{\rho}{\hat{\rho}_j} + (1-\rho)log\frac{1-\rho}{1-\hat{\rho}_j}. \tag{5}$$

To prevent overfitting, a weight decay term is also added to the cost function of the (3) [32]. Then, the final cost function to achieve the sparsity target in the SDAE as follows:

$$J_{sparse}(\boldsymbol{w}, \boldsymbol{b}) = J(\boldsymbol{w}, \boldsymbol{b}) + \beta J_{KL}(\rho\|\hat{\rho}). \tag{6}$$

Where β controls the sparsity penalty term.

B. SOFTMAX REGRESSION MODEL USING FOR CLASSIFICATION

The softmax regression model is a supervised learning algorithm and is widely used during the supervised learning steps of deep neural networks (DNN). Once the extraction of ECG feature representation is complete, we add a softmax regression layer on the top of the resulting hidden representation layers to classify the ECG beat. Then the back-propagation is used to fine tune the entire DNN by minimizing the following cost function:

$$J(\boldsymbol{\theta}_{DNN}) = -\frac{1}{n}\sum_{i=1}^{n}\sum_{k=1}^{K}1\left(\boldsymbol{y}_i = k\right)\log\left(\frac{\exp(\boldsymbol{h}_{\boldsymbol{\theta}_{DNN}}(\boldsymbol{x}_i)}{\sum_{k=1}^{K}\exp\left(\boldsymbol{h}_{\boldsymbol{\theta}_{DNN}}(\boldsymbol{x}_i)\right)}\right) + \frac{\gamma}{2}\left(\left\|\boldsymbol{W}_{softmax}\right\|_F^2 + \sum_{l=1}^{H}\|\boldsymbol{W}_l\|_F^2\right). \tag{7}$$

Where the first term is the cross-entropy loss for the softmax layer; the second term is the weight decay penalty; and the $\boldsymbol{h}_{\boldsymbol{\theta}_{DNN}}(\boldsymbol{x}_i)$ is the output of the DNN for an input $\boldsymbol{x}_i$. And $1\{\cdot\}$ is the indicator function, in other words, 1{a true statement} = 1, and 1{a false statement} = 0.

C. ACTIVE LEARNING FOR FINE TUNING

In this paper, we use active learning to fine tune the DNN and reduce the need for large amounts of labeled samples. The basic concept of active learning is requested an expert to label the most relevant new samples from the unlabeled set, and then adds the most relevant new samples to the train set. The most relevant question is how to select the most informative samples. To select the most informative samples, we use the method relies on the DNN posterior probabilities to associate confidence measures [28], [29]. We get the posterior probabilities according to Platt's method with the support vector machines (SVM) [33], [34]. Then two different sampling schemes, based on the posterior probabilities, are implemented: 1) (BT) algorithm [28] and MBT algorithm [29].

BT active learning algorithm is based on the posterior probabilities to achieve diversity in the sampling. In a multi-class setting, BT tries to improve the difference between the two highest posterior probabilities, thus improving the classification confidence. The decision criterion is

$$\hat{\boldsymbol{x}}_i^{BT} = \underset{x_i, i\in S_u}{\operatorname{argmax}} \left\{ \max_{k\in L} p\left(\boldsymbol{y}_i = k|\boldsymbol{x}_i\right) - \max_{k\in L\setminus\{k^+\}} p\left(\boldsymbol{y}_i = k|\boldsymbol{x}_i\right) \right\}. \tag{8}$$

where $s = \{1, 2, \ldots, n$ denotes a set of ECG heartbeats; the $L = \{1, 2, \ldots, K$ is the set of K labels; $\boldsymbol{x} = \{\boldsymbol{x}_1, \boldsymbol{x}_2, \ldots, \boldsymbol{x}_n \in R^{d\times n}$ denotes the d-dimensional feature vectors; $\boldsymbol{y} = \{\boldsymbol{y}_1, \boldsymbol{y}_2, \ldots, \boldsymbol{y}_n \in L^n$ is the set of ECG heartbeat labels; and $k^+ = \underset{k\in L}{\operatorname{argmax}}\, p\left(\boldsymbol{y}_i = k|\boldsymbol{x}_i\right)$ is the most probable class for sample $\boldsymbol{x}_i$.

To obtain more diversity in the composition of the training set, BT criterion focuses on the boundary region between two classes. Although the BT performance well, it may still induce biased sample when there are a large number of samples located close a boundary.

To promote the diversity in the sampling process, Li *et al.* [29] proposed the MBT active learning. For a given s $\in$ L , let $S_{U_s} \subset S_u$ be the set of samples such that $p\left(\boldsymbol{y}_i = s|\boldsymbol{x}_i\right) \geq p\left(\boldsymbol{y}_i = k|\boldsymbol{x}_i\right)$, for $i \in S_{U_s}$ and $s \neq k$. Then, the MBT criterion simply works as follows:

do
s = next class
select S_{U_s}

$$\hat{\boldsymbol{x}}_i^{MBT} = \underset{\boldsymbol{x}_i, i\in S_{U_s}, k\in L\setminus\{s\}}{\operatorname{argmax}} \left\{ p\left(\boldsymbol{y}_i = k|\boldsymbol{x}_i\right) \right\}, \tag{9}$$

while stop rule.

Where the ''next class'' is chosen by scanning the index set L in a cyclic fashion.

IV. EXPERIMENTAL RESULTS

A. DATASET DESCRIPTION

In this study, we used the well-known MIT-BIH arrhythmia database to perform the assessment of proposed approach to classify the ECG. Then we used the ECG data obtained from the wearable device to validate the performance of proposed approach. The details of the two databases are described as follows. Table 1 shows the class distribution in the two databases.

TABLE 1. The class distribution in the two databases.

Database	N	S	V	F	#REC
MIT-BIH	89821	3029	7037	813	44
WDDB	153676	2133	4284	327	65

1) MIT-BIH ARRHYTHMIA DATABASE (MIT-BIH)

This database contains 48 recordings, and each recording contains two-lead ECG signals for approximately 30-min long of 47 subjects. The ECG signals are band-pass filtered at 0.1-100 Hz and then sampled at 360 Hz. This database contains annotation for both timing information and beat class information confirmed by independent experts. In our study, 44 recordings (serial number: 101, 100, 103, 105, 106, 108, 109,111, 112, 113, 114, 115, 116, 117, 118, 119, 121, 122, 123, 124, 200, 201, 202, 203, 205, 207, 208, 209, 210, 212, 213, 214, 215, 219, 220, 221, 222, 223, 228, 230, 231, 232, 233, 234) from the MIT-BIH arrhythmia database are used, excluding 4 recordings (serial number: 102, 104, 107, 217), which contain paced heartbeats. The first 20 recordings (serial number: 100–124), which include representative samples of routine clinical records, are utilized to select representative beats to be included in the common training data. The remaining 24 used records (serial number: 200–234) contain uncommon but clinically important arrhythmias, such as ventricular, junctional, and supraventricular arrhythmias [35]–[37].

2) THE DATABASE OBTAINED FROM THE WEARABLE DEVICE (WDDB)

This database consists of 75 recordings of approximately 30 min and sampled at 200 Hz. These recordings were collected from 60 coronary artery disease patients (31 men and 29 women, age range 28 to 75 years). The beat type annotations of the recordings were performed by the 8000 Holter scanner and then reviewed and corrected by three medical students.

B. EXPERIMENTS SETUP AND PERFORMANCE EVALUATION

All of the ECG data in both of the two databases are preprocessed firstly. The preprocessing of the data includes filtering wave and denoising. All of the ECG signals are removed P wave and QRS complex by using a 200 ms width median filter. And the T wave is removed by a 600 ms width median filter. The original signals subtract the resulted signals to yield the baseline-corrected ECG signals. Then we remove the power-line and high-frequency noise by a 12-order low-pass filter with a 35Hz cut-off frequency.

Similar to [26] and [38], the training set contains the ECG from 22 recordings (101, 106, 108, 109, 112, 114, 115, 116,

TABLE 2. The results of classification in terms of VEB (11 testing records) and SVEB (14 testing records) of MIT-BIH.

Method	Labeled	SVEB				VEB			
		Acc	Ppr	Sen	Spe	Acc	Ppr	Sen	Spe
Chazal et al. [38]	500	0.959	0.470	0.877	Na	0.994	0.962	0.943	Na
Hu et al. [7]	300	Na	Na	Na	Na	0.948	0.758	0.789	0.968
Ince et al. [20]	300	0.961	0.634	0.818	0.985	0.979	0.922	0.903	0.988
Jiang et al. [21]	300	0.975	0.788	0.749	0.988	0.988	0.958	0.943	0.994
Kiranyaz et al. [26]	Na	0.964	0.792	0.686	0.995	0.989	0.962	0.959	0.994
BT	0	0.944	0.516	0.176	0.937	0.949	0.570	0.833	0.939
	50	0.969	0.791	0.821	0.967	0.971	0.851	0.951	0.972
	100	0.978	0.827	0.886	0.981	0.982	0.913	0.969	0.984
	200	0.991	0.912	0.914	0.995	0.994	0.957	0.974	0.995
	300	0.997	0.951	0.975	0.999	0.998	0.987	0.983	0.999
MBT	50	0.966	0.862	0.819	0.977	0.975	0.831	0.956	0.974
	100	0.975	0.887	0.873	0.985	0.984	0.887	0.971	0.985
	200	0.987	0.919	0.921	0.993	0.993	0.936	0.976	0.994
	300	0.997	0.957	0.972	0.999	0.998	0.984	0.981	0.999

118, 119, 122, 124, 201, 203, 205, 207, 208, 209, 215, 220, 223, 230). To evaluate the performance of the proposed approach, the testing set includes both MIT-BIH database and the ECG data obtained from the wearable device. We present the results in term of VEB (V class versus [N, S, and F]) and SVEB (S class versus [N, V, and F]) [18]. For MIT-BIH database, we access the performance into three evaluation datasets for building the test set: 1) using 11 test records (200, 202, 210, 213, 214, 219, 221, 228, 231, 233, and 234) for VEB detection and 14 test records (with the addition of records 212, 222, and 232) for SVEB detection; 2) using 24 test recordings from 200 up to 234; and 3) using all of the 44 recordings.

In order to achieve a suitable feature representation of the ECG data, we use ECG morphology features and two temporal features [18], [38]. We select the ECG morphology features 100 ms before the R-peak and 450 ms after the R-peak. The two temporal features are: 1) the Pre-RR interval feature which is the distance between a current R-peak and its previous R-peak; 2) the Post-RR interval feature representing the distance between the current R-peak and the next R-peak. To extract these feature, we detect the QRS by means of the well-known ecgpuwave software available on http://www.physionet.org/ physiotools/ecgpuwave/src/. As the sampling rate of MIT-BIH database is different from the sampling rate of the database obtained from the wearable device, we resample all segmented ECG signals to the same periodic length equal to 50 uniformly distributed samples. The length of the ECG feature vector including morphology and temporal features equals 52 for each beat.

The classification is evaluated using the standard measures: classification accuracy (Acc), sensitivity (Sen), specificity (Spe), and positive predictivity (Ppr) [18].

Since the range of sigmoid function is (0,1), we normalize the ECG feature vector in the range of (0,1) firstly. Then we pre-train the autoencoder. We setup the encoding part architecture with 52 nodes in visible layer and 200 nodes in hidden layer. The learning rate is 1. The epoch is 400, and the batchsize is 10. The denoising parameter is 0.5. After that, we initial the weight parameters to small values in the range (-0.005, 0.005) randomly. To fine tune the DNN, we use back-propagation algorithm. In the active learning phase, we get the posterior probabilities using a 10-fold cross-validation technique in the range (0, 0.5). We carry out the experiments on a desktop with the following configuration: core i7, CPU 3.6 GHz, RAM 16 GB, and GPU Nvidia Quadro K620 2G.

C. THE RESULTS ON MIT-BIH DATABASE

Table 2 shows the result of classification in terms of VEB (11 testing records) and SVEB (14 testing records) of MIT-BIH database. When the active learning is not used in the fine tune phase, the value of Acc, Ppr, Sen and Spe for SVEB are 94.4%, 51.6%, 17.6% and 93.7%, respectively. And the value of Acc, Ppr, Sen and Spe for VEB are 94.9%, 57.0%, 83.3% and 93.9%, respectively. Although the Acc and Spe are quite high, the Ppr and Sen are quiet low, especially for SVEB. When we add the active learning in the fine tune phase, all of the four values are improved, especially the Ppr and Sen. And these four values are increased with the increase of the number of samples from the testing set to the training set both in BT and MBT methods. And when the number of samples increase to 300, all of these four values have reached a quiet high level.

Table 3 and table 4 show the results of classification in terms of VEB and SVEB using 24 testing records and 44 testing records of MIT-BIH database, respectively. Similar to table 2, the values of Acc, Ppr, Sen and Spe are also quite low when the active learning is not added in the fine tune phase, in terms of VEB and SVEB using 24 testing records and 44 testing records of MIT-BIH database. When the active

TABLE 3. The results of classification in terms of VEB and SVEB using 24 testing records of MIT-BIH.

Method	Labeled	SVEB				VEB			
		Acc	Ppr	Sen	Spe	Acc	Ppr	Sen	Spe
Ince et al. [20]	300	0.961	0.567	0.621	0.985	0.976	0.874	0.834	0.981
Jiang et al. [21]	300	0.966	0.679	0.506	0.988	0.981	0.933	0.866	0.993
Kiranyaz et al. [26]	Na	0.964	0.621	0.646	0.986	0.986	0.895	0.95	0.981
BT	0	0.969	0.643	0.337	0.943	0.950	0.666	0.927	0.949
	50	0.981	0.814	0.897	0.973	0.981	0.886	0.958	0.969
	100	0.991	0.834	0.916	0.986	0.991	0.915	0.971	0.982
	200	0.995	0.913	0.953	0.994	0.993	0.962	0.978	0.994
	300	0.997	0.950	0.971	0.998	0.997	0.986	0.981	0.998
MBT	50	0.976	0.875	0.821	0.974	0.978	0.821	0.953	0.971
	100	0.989	0.891	0.867	0.989	0.989	0.873	0.969	0.983
	200	0.994	0.921	0.934	0.995	0.992	0.946	0.973	0.992
	300	0.997	0.956	0.961	0.999	0.995	0.973	0.979	0.997

TABLE 4. The results of classification in terms of VEB and SVEB using 44 testing records of MIT-BIH.

Method	Labeled	SVEB				VEB			
		Acc	Ppr	Sen	Spe	Acc	Ppr	Sen	Spe
Ince et al. [20]	300	0.974	0.537	0.632	0.990	0.983	0.874	0.846	0.987
Kiranyaz et al.[26]	Na	0.976	0.635	0.603	0.992	0.990	0.906	0.939	0.989
BT	0	0.972	0.628	0.462	0.949	0.961	0.705	0.933	0.952
	50	0.994	0.810	0.899	0.995	0.993	0.917	0.975	0.993
	100	0.995	0.851	0.923	0.996	0.994	0.928	0.981	0.994
	200	0.997	0.917	0.957	0.998	0.996	0.956	0.987	0.997
	300	0.998	0.953	0.985	0.999	0.998	0.984	0.994	0.999
MBT	0	0.972	0.628	0.462	0.949	0.961	0.705	0.933	0.952
	50	0.984	0.881	0.835	0.994	0.991	0.835	0.972	0.989
	100	0.985	0.887	0.884	0.995	0.994	0.887	0.979	0.994
	200	0.988	0.911	0.949	0.997	0.996	0.956	0.986	0.997
	300	0.998	0.951	0.987	0.999	0.999	0.983	0.992	0.999

learning is added in the fine tune phase, all of the four values are increased, especially the Ppr and Sen. The results in tables 2-4 confirm that the performance of our proposed method is better than the state-of-the-art methods.

Fig. 3 and Fig. 4 show the results of the classification for SVEB and VEB using 44 records of MIT-BIH database with different numbers of queries in both BT method and MBT method. For each query, the expert labels 10 ECG beats from the test set, and then these labeled beats are added to the training set to update the weight of the SDAE through back-propagation. As the figures shown, all of the four parameters are increased with the increase of the queries. After 10 queries, all of the four parameters reach a quiet high level for SVEB and VEB in both BT method and MBT method.

D. THE RESULTS ON WDDB DATABASE

To estimate the generalization ability of the proposed approach, we repeat the experiments on the WDDB database. As mentioned in the 4.2 section, we use 22 records of MIT-BIT database as the training set, and use the WDDB database as the test set. The results of classification in terms of SVEB and VEB using testing records of WDDB database are shown in table 5. As the table 5 shown, the values of Acc, Ppr, Sen and Spe do not perform well without the active learning in the fine phase both for SVEB (92.2%, 43.1%, 42.5% and 92.9%, respectively) and for VEB (93.3%, 52.1%, 49.2% and 93.1%, respectively). When the active learning is added in the fine tune phase, the values of Ppr and Sen are meliorated on a large extent. After adding 300 samples in BT method, the four parameters reach 99.8%, 95.8%, 93.7% and 99.9% for SVEB, and 99.8%, 98.3%, 97.4% and 99.9% for VEB. Similarly, when 300 samples are added in MBT method, the four parameters are up to 99.8%, 95.3%, 94.3% and 99.9% for SVEB, and 99.8%, 98.4%, 98.2% and 99.9% for VEB. Fig. 5 and Fig. 6 show that the four parameters vary with the number of the queries for SVEB and VEB, respectively.

TABLE 5. The results of classification in terms of VEB and SVEB using testing records of WDDB database.

Method	Labeled	SVEB				VEB			
		Acc	Ppr	Sen	Spe	Acc	Ppr	Sen	Spe
BT	0	0.922	0.431	0.425	0.929	0.933	0.521	0.492	0.931
	50	0.981	0.781	0.793	0.955	0.985	0.935	0.923	0.961
	100	0.993	0.845	0.907	0.987	0.993	0.955	0.947	0.987
	200	0.996	0.917	0.931	0.994	0.996	0.971	0.965	0.995
	300	0.998	0.958	0.937	0.999	0.998	0.983	0.974	0.999
MBT	50	0.971	0.826	0.832	0.953	0.969	0.876	0.913	0.949
	100	0.991	0.883	0.903	0.977	0.989	0.945	0.937	0.971
	200	0.995	0.927	0.932	0.993	0.995	0.981	0.968	0.996
	300	0.998	0.953	0.943	0.999	0.998	0.984	0.982	0.999

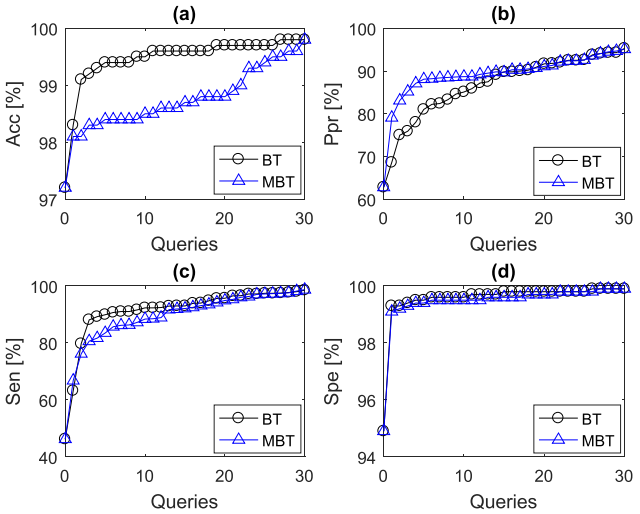

FIGURE 3. The results of classification in terms of SVEB using 44 testing records of MIT-BIH.

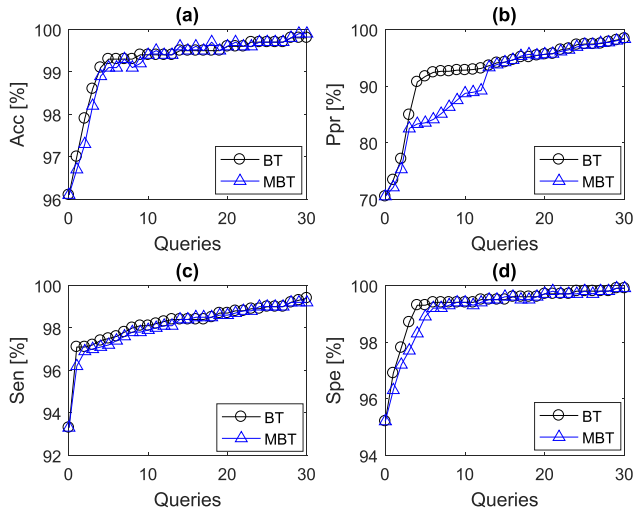

FIGURE 4. The results of classification in terms of VEB using 44 testing records of MIT-BIH.

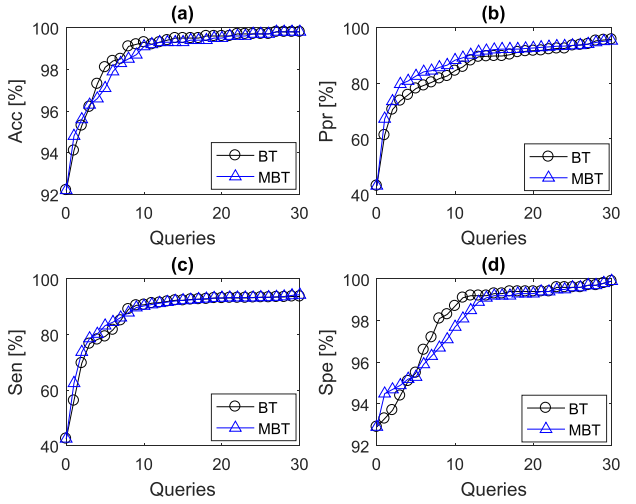

FIGURE 5. The results of classification in terms of SVEB on the WDDB dataset.

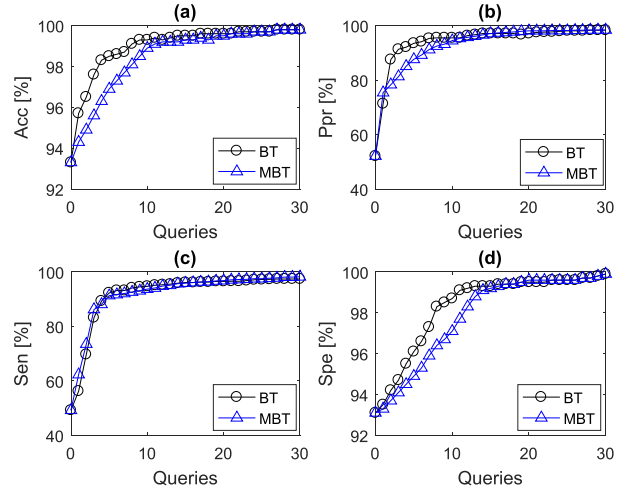

FIGURE 6. The results of classification in terms of VEB on the WDDB dataset.

E. THE RESULTS OF THE CLASSIFICATION WITH DIFFERENT LAYERS ON BT METHOD

To explore influence of the layers of the DNN on the performance of the proposed method, we repeat the above experiments with configuration of different hidden layers. We set the number of hidden layers to 2, 3, 4, and use {200, 100}, {200, 100, 200} and {200, 100, 200, 100} nodes in each hidden layer, respectively. Fig. 7 and Fig. 8 show the results

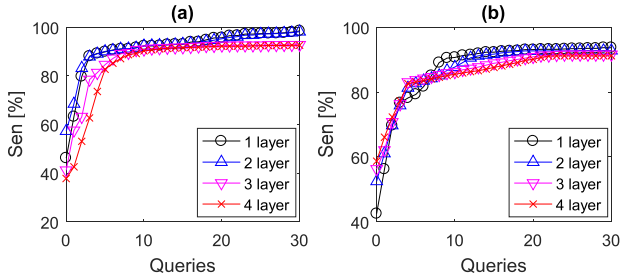

FIGURE 7. The classification results in terms of SVEB obtained by BT method with multiple hidden layers on: (a) 44 recordings of MIT-BIH and (b) WDDB database.

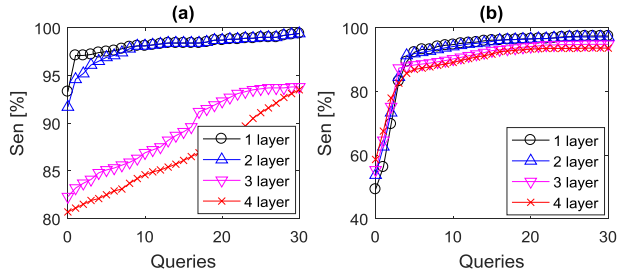

FIGURE 8. The classification results in terms of VEB obtained by BT method with multiple hidden layers on: (a) 44 recordings of MIT-BIH and (b) WDDB database.

on different hidden layers on the two databases. The results show that one and two hidden layers in the DNN have better performance. And we find that the performance of the DNN does not improve along with the number of the hidden layers increased.

V. DISCUSSION

In this study, a deep neural network (DNN) is proposed to classify the ECG signals automatically. We learn a suitable feature representation using SDAE with sparity constraint. In order to classify the ECG signals, the learned feature representation is fed to a softmax regression. To fine tune the DNN, the active learning is used in the fine-tuning phase. We apply the DNN on the well-known MIT-BIH database and the database obtained from the wearable device. To assess the results of the proposed method, Acc, Ppr, Sen and Spe are used to evaluate the performance. Our results show that the generalization capabilities of the DNN proposed in this paper are acceptable.

In our experiments, we compare our proposed approach with adaptive system [38], ''mixture-of-experts'' (MOE) approach [7], using feature extraction based on principal component analysis (PCA) [20], Block-based neural networks [19] and 1-D CNN [26]. Chazal and Reilly [38] used MIT-BIH database to evaluate their adaptive system. As the table 2 shown, when they added 500 samples in the adaptive system, the Acc, Ppr and Sen reached 95.9%, 47% and 87.7% for SVEB and 99.4%, 96.2% and 94.3% for SVEB, respectively. Their results are close to our results in terms of VEB, but our results outperform their results for SVEB. Hu et al. used ''mixture-of-experts'' (MOE) approach [7] to classify 11 recordings of MIT-BIH database for VEB. Our results (99.8%, 98.7%, 98.3% and 99.9% on BT) exceeds their results (Acc 94.8%, Ppr 75.8%, Sen 78.9% and Spe 96.8%). Ince *et al.* [20] extracted the feature representation using wavelet transform and PCA, and then they classified the ECG by artificial neural networks. Our results surpass their results in all of the three evaluation datasets on the MIT-BIH database. Jiang and Kong [19] utilized the block-based neural networks to classify the ECG signals and elevated the results on MIT-BIH database. As the table 2 and table 3 shown, our results outperform the results in their experiments. 1-D CNN was used for both feature extraction and classification of the ECG data on MIT-BIH database [26]. In all of the three evaluation datasets on the MIT-BIH database, our results are better than their results. The results show that our approach outperforms the state-of-the-art methods. Moreover, we also elevate our approach on the ECG data obtained from the wearable device. We use 22 recordings of MIT-BIT to train the model, and in the fine-tuning phase, we add active learning. When 300 samples are added into the training set from the WDDB, the results of the classification also reach excellent level.

The active learning procedure seriously plays a significant role in improving the performance of ECG classification. In both the MIT-BIH database and the database obtained from the wearable device, we use the SDAE to learn a suitable feature representation of the ECG beat signals and classify them with softmax regression. When the active learning procedure is not added in the fine tune phase, although the Acc and Spe present well, the Sen and Ppr are quite low both for SVEB and for VEB in the two databases. However, when the active learning procedure is added in the fine tune phase, the performance of the classification is improved clearly, especially the Sen and Ppr. Active learning reduces the experts' labeling efforts in classifying the ECG signals. In order to select the most useful samples that can improve the model, BT [28] and MBT [29] methods are used in the active learning phase. Both of the two methods try to find the most ambiguous samples and give them to an expert for labeling. Then these labeled samples are used to retrain the classification model. Both BT and MBT are based on DNN posterior probabilities. In the BT method, the difference between the two DNN posterior probabilities is calculated. When the difference is small, it implies the classification confidence is low. Then the samples with low difference are selected for labeling. As the BT criterion focused on the boundary region between two classes, it may produce biased sampling when there are a large number of samples located close to a boundary. So we add the MBT criterion in the active learning phase. Our results show that both BT and MBT criterions obtain a quiet outstanding performance.

Indeed, the active learning improves the model performance. As a cost, it also increases the computational complexity of the system. In the active learning phase, the training process need provide posterior probabilities. To get the posterior probabilities, we train SVM according to Platt's method [33], [34]. When we train SVM, we select

radial basis function as the kernel function and use grid search method to get the suitable parameters. Then we use BT and MBT criterions to select the most useful samples from the test set and then add these samples to the training set. After that, we utilize SDAE with sparsity constraint to learn an adequate feature representation and classify the ECG signals according to the AAMI standard by the softmax regression layer. Both training SVM and training SDAE enhance the computational complexity of the system.

Furthermore, we also investigate whether the number of hidden layers of the DNN has an impact on performance of the proposed method. As Fig. 7 and Fig. 8 shown, when we increase the hidden layers, the performance of our proposed approach does not improve. On the contrary, the performance of the model is reduced with the increase of hidden layers. On the other hand, the increase of hidden layers also raises the computational complexity of the system.

Notwithstanding the performance of our study is outstanding, we should interpret the limitations of our study. Firstly, the preprocessing of the ECG signals is simple. We just use median filter to remove the noise, and use low-pass filter to eliminate the power-line and high-frequency noise. When the signal noise is not serious, the simple method can play the role of filtering. However, when the noise is intricate, this method is difficult to eliminate noise effectively. Then it can have an adverse effect of the subsequent ECG feature extraction. Moreover, we only use morphology and temporal features as the feature vector. This method ignores the feature values of ECG signal in the frequency domain, and it may result in loss some useful information. Although the fact that the results are very outstanding, we believe that there is still a space for improving the performance by using other deep learning techniques and more feature representation both in time domain and frequency domain. We leave these methods as future work.

VI. CONCLUSION

In this study, an automatic wearable ECG classification and monitoring system with SDAE is presented. We use SDAE to learn the ECG feature representation, and classify the ECG beat by softmax regression. To elevate the performance of the system, active learning is added in the fine tuning of the DNN. In the active learning, the most informative samples are selected by BT and MBT methods. The results of the classification on the MIT-BIH arrhythmia database show that both the SVEB and the VEB detections outperform the most of state-of-the-art methods. Moreover, on the WDDB database, it also has an outstanding performance. It suggests that the proposed approach is an effective and robust method to classify the ECG signals.

REFERENCES

[1] B. J. Maron *et al.*, "Assessment of the 12-lead ECG as a screening test for detection of cardiovascular disease in healthy general populations of young people (12–25 years of age) a scientific statement from the American Heart Association and the American College of Cardiology," *Circulation*, vol. 130, no. 15, pp. 1303–1334, Sep. 2014.

[2] R. Auer *et al.*, "Association of major and minor ECG abnormalities with coronary heart disease events," *JAMA*, vol. 307, no. 14, pp. 1497–1505, Apr. 2012.

[3] S. Pandey, W. Voorsluys, S. Niu, A. Khandoker, and R. Buyya, "An autonomic cloud environment for hosting ECG data analysis services," *Future Generat. Comput. Syst.*, vol. 28, no. 1, pp. 147–154, Jan. 2012.

[4] J. A. Walsh, E. J. Topol, and S. R. Steinhubl, "Novel wireless devices for cardiac monitoring," *Circulation*, vol. 130, no. 7, pp. 573–581, Aug. 2014.

[5] K. Minami, H. Nakajima, and T. Toyoshima, "Real-time discrimination of ventricular tachyarrhythmia with Fourier-transform neural network," *IEEE Trans. Biomed. Eng.*, vol. 46, no. 2, pp. 179–185, Feb. 1999.

[6] S. Kiranyaz, T. Ince, J. Pulkkinen, and M. Gabbouj, "Personalized long-term ECG classification: A systematic approach," *Expert Syst. Appl.*, vol. 38, no. 4, pp. 3220–3226, Apr. 2011.

[7] Y. H. Hu, S. Palreddy, and W. J. Tompkins, "A patient-adaptable ECG beat classifier using a mixture of experts approach," *IEEE Trans. Biomed. Eng.*, vol. 44, no. 9, pp. 891–900, Sep. 1997.

[8] J. Fayn, "A classification tree approach for cardiac ischemia detection using spatiotemporal information from three standard ECG leads," *IEEE Trans.Biomed. Eng.*, vol. 58, no. 1, pp. 95–102, Jan. 2011.

[9] L. Pecchia, P. Melillo, and M. Bracale, "Remote health monitoring of heart failure with data mining via CART method on HRV features," *IEEE Trans. Biomed. Eng.*, vol. 58, no. 3, pp. 800–804, Mar. 2011.

[10] Y. H. Hu, W. J. Tompkins, J. L. Urrusti, and V. X. Afonso, "Applications of artificial neural networks for ECG signal detection and classification," *J. Electrocardiol.*, vol. 26, pp. 66–73, Jan. 1993.

[11] D. A. Coast, R. M. Stern, G. G. Cano, and S. A. Briller, "An approach to cardiac arrhythmia analysis using hidden Markov models," *IEEE Trans. Biomed. Eng.*, vol. 37, no. 9, pp. 826–836, Sep. 1990.

[12] S. Osowski, T. Hoai, and T. Markiewicz, "Support vector machine-based expert system for reliable heartbeat recognition," *IEEE Trans.Biomed. Eng.*, vol. 51, no. 4, pp. 582–589, Apr. 2004.

[13] J.-S. Wang, W.-C. Chiang, Y.-L. Hsu, and Y.-T. C. Yang, "ECG arrhythmia classification using a probabilistic neural network with a feature reduction method," *Neurocomputing*, vol. 116, pp. 38–45, Sep. 2013.

[14] E. D. Ibeyli, "Recurrent neural networks employing Lyapunov exponents for analysis of ECG signals," *Expert Syst. Appl.*, vol. 37, no. 2, pp. 1192–1199, Mar. 2010.

[15] E. J. da S. Luz, T. M. Nunes, V. H. C. De Albuquerque, J. P. Papa, and D. Menotti, "ECG arrhythmia classification based on optimum-path forest," *Expert Syst. Appl.*, vol. 40, no. 9, pp. 3561–3573, Jul. 2013.

[16] R. Hoekema, G. J. H. Uijen, and A. van Oosterom, "Geometrical aspects of the interindividual variability of multilead ECG recordings," *IEEE Trans. Biomed. Eng.*, vol. 48, no. 5, pp. 551–559, May 2001.

[17] *Recommended Practice for Testing and Reporting Performance Results of Ventricular Arrhythmia Detection Algorithms*, Assoc. Adv. Med. Instrum., Arlington, VA, USA, 1987.

[18] P. de Chazal, M. O'Dwyer, and R. B. Reilly, "Automatic classification of heartbeats using ECG morphology and heartbeat interval features," *IEEE Trans. Biomed. Eng.*, vol. 51, no. 7, pp. 1196–1206, Jul. 2004.

[19] W. Jiang and S. G. Kong, "Block-based neural networks for personalized ECG signal classification," *IEEE Trans. Neural Netw.*, vol. 18, no. 6, pp. 1750–1761, Nov. 2007.

[20] T. Ince, S. Kiranyaz, and M. Gabbouj, "A generic and robust system for automated patient-specific classification of ECG signals," *IEEE Trans. Biomed. Eng.*, vol. 56, no. 5, pp. 1415–1426, May 2009.

[21] M. Llamedo and J. P. Martínez, "An automatic patient-adapted ECG heartbeat classifier allowing expert assistance," *IEEE Trans. Biomed. Eng.*, vol. 59, no. 8, pp. 2312–2320, Aug. 2012.

[22] G. E. Hinton, S. Osindero, and Y.-W. Teh, "A fast learning algorithm for deep belief nets," *Neural Comput.*, vol. 18, no. 7, pp. 1527–1554, 2006.

[23] J. Schmidhuber, "Deep learning in neural networks: An overview," *Neural Netw.*, vol. 61, pp. 85–117, Jan. 2015.

[24] P. Swietojanski, A. Ghoshal, and S. Renals, "Convolutional neural networks for distant speech recognition," *IEEE Signal Process. Lett.*, vol. 21, no. 9, pp. 1120–1124, Sep. 2014.

[25] M. Huanhuan and Z. Yue, "Classification of electrocardiogram signals with deep belief networks," in *Proc. IEEE 17th Int. Conf. Comput. Sci. Eng.*, Chengdu, China, Dec. 2014, pp. 7–12.

[26] S. Kiranyaz, T. Ince, and M. Gabbouj, "Real-time patient-specific ECG classification by 1-D convolutional neural networks," *IEEE Trans. Biomed. Eng.*, vol. 63, no. 3, pp. 664–675, Mar. 2016.

[27] R. M. Castro and R. D. Nowak, "Minimax bounds for active learning," *IEEE Trans. Inf. Theory*, vol. 54, no. 5, pp. 2339–2353, May 2008.
[28] T. Luo *et al.*, "Active learning to recognize multiple types of plankton," *J. Mach. Learn. Res.*, vol. 6, pp. 589–613, Apr. 2005.
[29] J. Li, J. M. Bioucas-Dias, and A. Plaza, "Hyperspectral image segmentation using a new Bayesian approach with active learning," *IEEE Trans. Geosci. Remote Sens.*, vol. 49, no. 10, pp. 3947–3960, Oct. 2011.
[30] L. Cao, W.-B. Huang, and F.-C. Sun, "Building feature space of extreme learning machine with sparse denoising stacked-autoencoder," *Neurocomputing*, vol. 174, pp. 60–71, Jan. 2016.
[31] H. Lee, C. Ekanadham, and A. Y. Ng, "Sparse deep belief net model for visual area V2," in *Proc. Neural Inf. Process. Syst.*, 2008, pp. 873–880.
[32] E. Hosseini-Asl, J. M. Zurada, and O. Nasraoui, "Deep learning of part-based representation of data using sparse autoencoders with nonnegativity constraints," *IEEE Trans. Neural Netw. Learn. Syst.*, vol. 27, no. 12, pp. 2486–2498, Dec. 2016.
[33] J. C. Platt, "Probabilistic outputs for support vector machines and comparisons to regularized likelihood methods," in *Advances in Large Margin Classifiers*. Cambridge, MA, USA: MIT Press, 1999, pp. 61–74.
[34] H.-T. Lin, C.-J. Lin, and R. C. Weng, "A note on Platt's probabilistic outputs for support vector machines," *Mach. Learn.*, vol. 68, no. 3, pp. 267–276, 2007.
[35] M. Llamedo and J. P. Martínez, "Heartbeat classification using feature selection driven by database generalization criteria," *IEEE Trans. Biomed. Eng.*, vol. 58, no. 3, pp. 616–625, Mar. 2011.
[36] A. L. Goldberger *et al.*, "PhysioBank, PhysioToolkit, and PhysioNet: Components of a new research resource for complex physiologic signals," *Circulation*, vol. 101, no. 23, pp. e215–e220, Jun. 2000.
[37] G. B. Moody and R. G. Mark, "The impact of the MIT-BIH arrhythmia database," *IEEE Eng. Med. Biol. Mag.*, vol. 20, no. 3, pp. 45–50, May/Jun. 2001.
[38] P. de Chazal and R. B. Reilly, "A patient-adapting heartbeat classifier using ECG morphology and heartbeat interval features," *IEEE Trans. Biomed. Eng.*, vol. 53, no. 12, pp. 2535–2543, Dec. 2006.

YUFA XIA received the B.S. degree in electronic and information engineering from the Huanghe Science and Technology College, Zhengzhou, China, in 2012, and the M.E. degree in electronics and communication engineering from Guizhou University, Guiyang, China, in 2015. He is currently a Research Assistant with the Shenzhen Institutes of Advanced Technology, Chinese Academy of Sciences, Shenzhen, China. His research interests include physiological signal analysis, medical image processing, and machine learning.

HUAILING ZHANG received the B.S. degree from Jiangxi Normal University, Nanchang, China, in 1983. He is currently a Professor with the Guangdong Medical University, Dongguan, China. His research interests include physiological signal analysis and medical image processing.

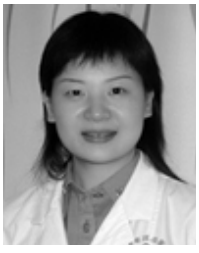

LIN XU is currently a Cardiologist with the General Hospital of Guangzhou Military Command of PLA, Guangzhou, China. Her research focuses on cardiovascular disease.

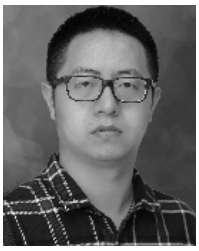

ZHIFAN GAO (M'18) received the B.S. and M.E. degrees in electronics and information engineering from the Huazhong University of Science and Technology, Wuhan, China, in 2009 and 2011, respectively, and the Ph.D. degree in pattern recognition and intelligent systems from the University of Chinese Academy of Sciences, China, in 2017.

He is currently a Post-Doctoral Fellow with the Shenzhen Institutes of Advanced Technology, Chinese Academy of Sciences, Shenzhen, China. His research focuses on medical image processing, computer vision, and machine learning.

HEYE ZHANG (M'17) received the B.S. and M.E. degrees from Tsinghua University, Beijing, China, in 2001 and 2003, respectively, and the Ph.D. degree from the Hong Kong University of Science and Technology, Hong Kong, in 2007.

He is currently a Professor with the Shenzhen Institutes of Advanced Technology, Chinese Academy of Sciences, Shenzhen, China. He is also with the Key Laboratory for Health Informatics of the Chinese Academy of Sciences, China. His research interests include cardiac electrophysiology and cardiac image analysis.

HUAFENG LIU received the B.S. degree in optical engineering, the M.S. degree in measurement techniques and instruments, and the Ph.D. degree in positron emission tomography from the Department of Optical Engineering, Zhejiang University, China, 1995, 1998, and 2001, respectively.

He was a Post-Doctoral Fellow with the Hong Kong University of Science and Technology, China, from 2001 to 2003, with a focus on statistical filtering and inverse mechanics strategies for cardiac image analysis and PET image reconstruction. He is currently a Full Professor with Zhejiang University. He is the Director of the ZJU-HAMAMATSU Joint Photonics Lab, which was co-founded by Hamamatsu Photonics K. K. and the Department of Optic-Electronic Information Engineering, Zhejiang University, in 1995, where he has been focusing on biomedical imaging instrumentation (PET), image reconstruction (PET, fMRI, and ECG), and medical image analysis, since 1995.

SHUO LI received the Ph.D. degree from Concordia University, Canada, in 2006. He is currently a Professor with Western University, London, ON, Canada . He has published over 100 papers in top international journals and conferences, such as TPAMI, MIA, TNNLS, TMI, and CVPR. His research interests include cardiac electrophysiology and cardiac image analysis. He is a member of MICCAI Society Board, a Research Fellow of the Lawson Institute of Health, and a member of the IEEE Engineering in Medicine and Biology Society Transnational Engineering and Healthcare Innovation Technology Committee. He is the Deputy Editor of the *Medical Image Analysis* and the *Computerized Medical Imaging and Graphics* (CMIG). He is also the Guest Editor of the TMI, CMIG, and CVIU.